A Family of PWM plus Phase-Shift Bidirectional DC-DC Converters

Haifeng Fan, Dehong Xu
College of Electrical Engineering, Zhejiang University, Hangzhou, P. R. China
Email: xdh@cee.zju.edu.cn

***Abstract*—PWM is introduced to phase-shift bidirectional DC-DC converters, which can reduce current stresses, conduction loss and switching loss of semiconductors and can expand ZVS range. A technique to synthesize PWM plus phase-shift bidirectional DC-DC converter topologies is presented. Theoretical analysis, simulation and experimental results of one particular converter taken as an example, are provided in this paper.**

I. INTRODUCTION

Bidirectional DC-DC converters are expected to be candidates for applications such as DC-UPS, energy management, and auxiliary power supplies in electric vehicles [1-2].

Recently, bidirectional DC-DC converters were investigated, aiming at minimizing the size and weight of bidirectional DC-DC converters and EMI through soft-switching method [3-5]. Phase-Shift (PS) bidirectional DC-DC converter is attractive since it can realize ZVS without auxiliary switches. However it has high current stresses and narrow ZVS range when the amplitude of input voltage is not matched with that of output voltage. The authors have proposed PWM plus phase-shift bidirectional DC-DC converter, which features reduced current stress, conduction losses, switching losses of semiconductors and wide ZVS range [2]. Actually, PWM plus Phase-Shift Control (PPS) can be extended to a series of phase-shift bidirectional DC-DC converters.

In this paper, a technique to synthesize bidirectional DC-DC converters topologies is presented. Theoretical analysis, simulation and experimental results of one particular converter, are given.

II. OPERATION PRINCIPLE OF PPS BIDIRECTIONAL DC-DC CONVERTERS

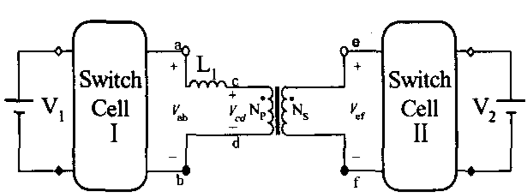

Fig.1. Conventional phase-shift bidirectional DC-DC converters

The block figure of conventional phase-shift bidirectional DC-DC converters is shown in Fig.1 [5].There are two switch cells on both sides of the isolation transformer. The leakage inductance of transformer is used as the main energy transfer element. Conceptual circuit of PS control is shown in Fig.2a, and that of PPS control is shown in Fig.2b. The PWM control of duty cycles can be seen as an electric transformer which regulates the amplitudes of equivalent input voltage (V_{ab}) and equivalent output voltage (V_{cd}), so that both positive and negative amplitudes of the equivalent input voltage (V_{ab}) are equal to those of the equivalent output voltage (V_{cd})[2].

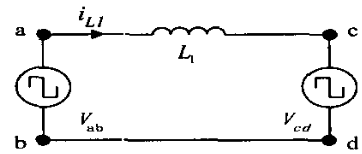

Fig.2a. Conceptual circuit of PS control

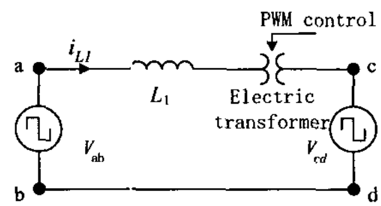

Fig.2b. Conceptual circuit of PPS control

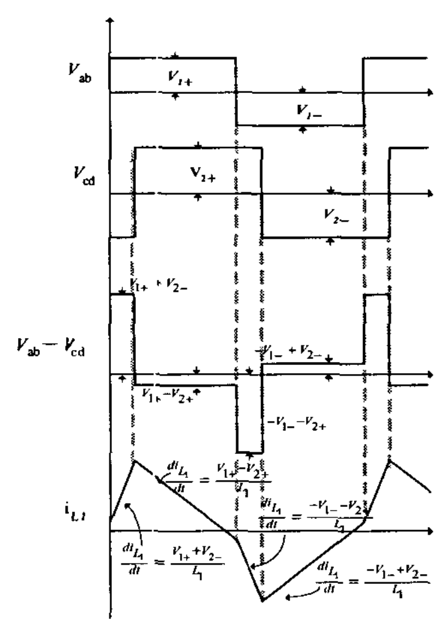

Fig.3a. Waveforms of PS control

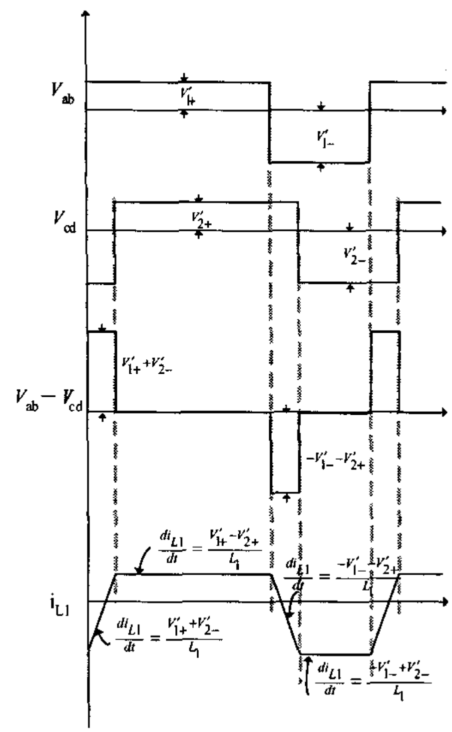

Fig.3b. Waveforms of PPS control

Fig.3a shows waveforms of PS control when the amplitude of equivalent input voltage (V_{ab}) is not equal to that of the equivalent output voltage (V_{cd}), such as $V_{1+} < V_{2+}$. Fig.3b show waveforms of PPS control .They have the same input voltage (V_1) and output voltage (V_2), but different duty cycle (D).

Compared with PS control, PPS control can reduce the current stresses and RMS currents of the converter. Thus losses of the converter can be decreased. Besides these, PPS can achieve ZVS in a larger load variation [2]. Therefore, it's necessary for us to find more topologies that can be controlled by PPS.

III. Generation of the Family of PPS Bidirectional DC-DC Converters

From the operation principle of PPS bidirectional DC-DC converters, we can find that bidirectional DC-DC converters which can be controlled by PPS should have the following features:

1. Switch cells used to synthesize PPS bidirectional DC-DC converters can be regarded as square-wave voltage source.
2. The amplitudes of square-wave voltage sources can be regulated by PWM.
3. Duty cycle can be varied so that both positive and negative amplitudes of the equivalent input voltage (V_{ab}) can always be equal to those of the equivalent output voltage (V_{cd}).

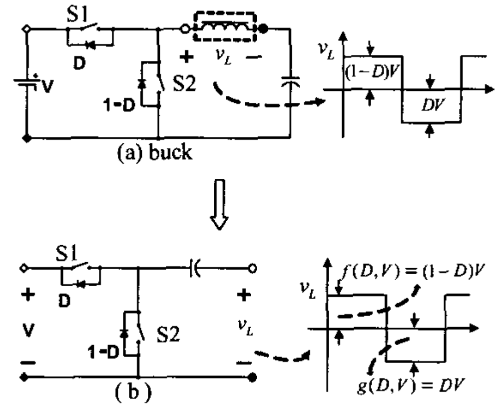

Fig.4. Generation of fundamental switch cell

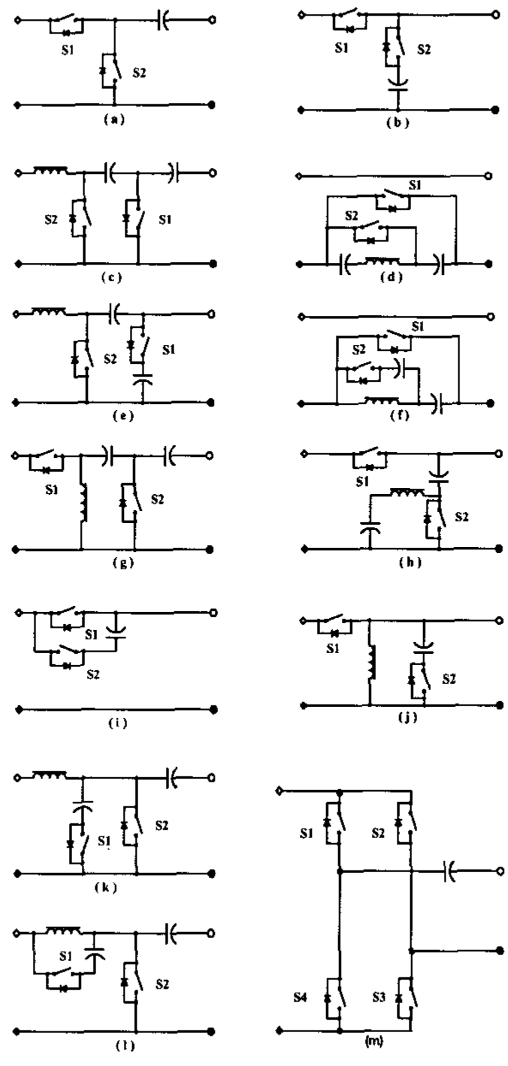

Fig.5. Switch cells of bidirectional DC-DC converters

A. Generation of switch cells

According to the voltage second balance of the inductors in DC-DC converters when they are in steady state, it can be found that the voltage waveforms across the inductors are square-wave on condition that the two switches operate in complementary mode .Therefore, the switch cells can be obtained from the fundamental bidirectional DC-DC converters [3]. Buck converter is taken as an example given in Fig.4. The voltage on inductor is square wave. When we move the inductor away as Fig.4 (b), we get a square-wave source, and the amplitudes of square-wave voltage source can be regulated by PWM. Fig.5 lists a family of switch cells. In switch cells (a)-(e), S1 and S2 operate in complementary mode. In full-bridge switch cell as shown in Fig.5 (m), S1 and S3 are driven by the same gate signal, and S2 and S4 are also driven by the same gate signal while S1 and S2 operate in complementary mode.

B. Synthesis of PPS bidirectional DC-DC converters

As a rule, the input port of a switch cell is connected to a voltage source (V), and the output port of a switch cell is connected with an inductor or a transformer as shown in Fig.1. The voltage waveform of the output port is square-wave. Its positive amplitude $f(\mathrm{D},V)$ and negative amplitude $g(\mathrm{D},V)$ can be derived, according the voltage second balance of output port connected inductor as Fig.4 (b). These switch cells listed in Figure 5 can be divided into three groups in terms of square-wave amplitudes of their output ports, and three groups are:

1) Group A switch cell (a), (m)
$f(D,V)=K_A(1-D)V$, $g(\mathrm{D},V)=K_A DV$

2) Group B switch cell (b), (c), (d), (f), (g), (h), (i), (j)
$f(D,V)=K_B V$, $g(D,V)=K_B DV/(1-D)$

3) Group C switch cell (e), (k), (l)
$f(D,V)=K_C(1-D)V/D$, $g(D,V)=K_C V$

Where D is the duty ratio of S1, K_A、K_B and K_c are constants as shown in TABLE I.

TABLE I

CONSTANT K

K \ SWITCH CELL	(a)	(m)	(b), (c), (d), (f) (g), (h), (i), (j)	(e), (k), (l)
K_A	1	2		
K_B			1	
K_C				1

In order to realize PPS control, the duty cycle D must be varied so that both positive and negative amplitudes of output of switch cell I are equal to those of switch cell II. Therefore, PPS control conditions can be summarized in equation (1).

$$\begin{cases} f_{\mathrm{I}}(\mathrm{D},V_1)=Nf_{\mathrm{II}}(\mathrm{D},V_2) \\ g_{\mathrm{I}}(\mathrm{D},V_1)=Ng_{\mathrm{II}}(\mathrm{D},V_2) \end{cases} \tag{1}$$

Where: N is the turn ratio of the transformer in Fig.1, $f_{\mathrm{I}}(D,V_1)$ is the positive amplitude of switch cell I output V_{ab}, $f_{II}(D,V_2)$ is the positive amplitude of switch cell II output V_{ef}, $g_{\mathrm{I}}(\mathrm{D},V_1)$ is the negative amplitude of switch cell I output V_{ab} , $g_{\mathrm{II}}(\mathrm{D},V_2)$ is the negative amplitude of switch cell II output V_{ef}.

For topologies shown in Fig.5, average voltages of switch cell output in one period are zero.

$$\begin{cases} Df_{\mathrm{I}}(\mathrm{D},V_1)-(1-D)g_{\mathrm{I}}(\mathrm{D},V_1)=0 \\ Df_{\mathrm{II}}(\mathrm{D},V_2)-(1-D)g_{\mathrm{II}}(\mathrm{D},V_2)=0 \end{cases} \tag{2}$$

From equation (2), we can get:

$$f_{\mathrm{I}}(\mathrm{D},V_1)/g_{\mathrm{I}}(\mathrm{D},V_1)=f_{\mathrm{II}}(\mathrm{D},V_2)/g_{\mathrm{II}}(\mathrm{D},V_2) \tag{3}$$

Therefore PPS control conditions equation (1) can be simplified as:

$$f_{\mathrm{I}}(\mathrm{D},V_1)=Nf_{\mathrm{II}}(\mathrm{D},V_2) \tag{4}$$

In other words, if D which can make equation (4) tenable is always existing for arbitrary V_1 and V_2, PPS control can be realized. D can be obtained as shown in TABLE II. Two switch cells belonging to different groups mentioned above can be used to build a PPS control bidirectional DC-DC converter. Fig.6 is a PPS control bidirectional DC-DC converter built by a switch cell belonging to group A and a switch cell belonging to group B. Fig.7 is a PPS control bidirectional DC-DC converter built by a switch cell belonging to group B and a switch cell belonging to group C.

TABLE II

VALUE OF D

SWITCH CELL I \ SWITCH CELL II (D)	A	B	C
A		$\frac{K_A V_2 - NK_B V_1}{K_A V_2}$	$\frac{NK_C V_2}{K_A V_1}$
B	$\frac{NK_A V_2 - K_B V_1}{NK_A V_2}$		$\frac{NK_C V_2}{K_B V_1 + NK_C V_2}$
C	$\frac{K_C V_1}{NK_A V_2}$	$\frac{K_C V_2}{NK_B V_1 + K_C V_2}$	

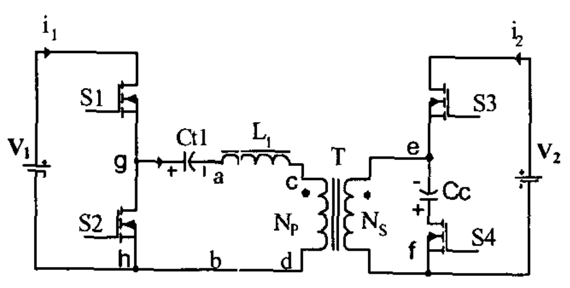

Fig.6 PPS control bidirectional DC-DC converter built by a switch cell belonging to group A and a switch cell belonging to group B.

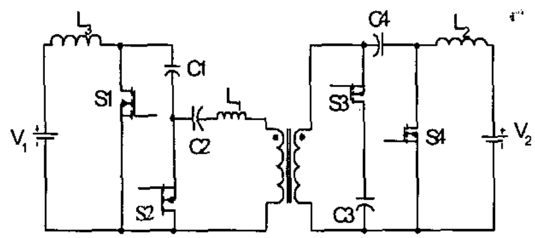

Fig.7 PPS control bidirectional DC-DC converter built by a switch cell belonging to group B and a switch cell belonging to group C

IV. Analysis of the Converter

As an example, cell (k) and cell (m) is combined to build a PPS bidirectional DC-DC converter shown in Fig.8. We select switch cell (k) from Group C as switch cell I, and select switch cell (m) from Group A as switch cell II. The positive amplitude of switch cell I output is $f_I(D,V_1)=(1-D)V_1/D$, and positive amplitude of switch cell II output is $f_{II}(D,V_2)=2(1-D)V_2$, then D can be derived from equation (4): $D=\frac{V_1}{2NV_2}$.

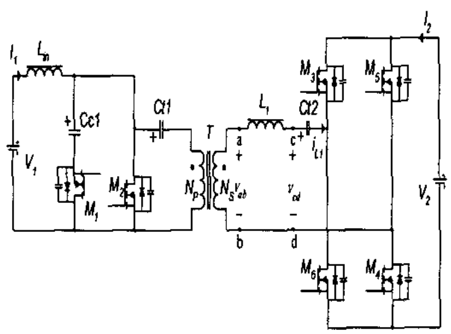

Fig.8. The proposed bidirectional DC-DC converter

To simplify the analysis, the operation of PPS control converter is explained with the following assumptions:

- The converter has reached steady state.
- All switch devices are assumed as ideal switches with parallel body diodes and parasitic capacitors.
- The inductance L_1 is composed of the leakage inductance of the transformer and additional series inductance.
- The values of the capacitors Ct1, Ct2, and Cc1 are so large that the voltage ripples across them are small.
- The resonant frequency of capacitor (composed of Ct1, Ct2, and Cc1) and L_1 is much lower than the switching frequency of the converter.

M_3 and M_4 are driven by the same gate signal, and M_5 and M_6 are also driven by the same gate signal. Duty cycles of M_1 and M_3 (M_4) is D, and duty cycles of M_2 and M_5 (M_6) is 1-D. In the forward mode, the gate drive signals of M_1 and M_2 have a leading phase compared to that of M_3 (M_4) and M_5 (M_6), and power flows from V_1 to V_2. The equivalent circuits and key waveforms are shown in Fig.9 and Fig.10, respectively. The switching cycle can be divided into 8 stages, which are explained below.

Stage 1 (t_0-t_1): Just before t_0, M_5 (M_6) is turned off. M_3 (M_4) is on. The current i_{L1} is in positive direction. The capacitor in parallel with M_5 (M_6) is charged, while the capacitor in parallel with M_3 (M_4) is discharged. The voltage across M_3 (M_4) decreases to zero at t_0 and M_3's body diode starts to conduct. M_3 (M_4) is turned on with ZVS and then works as a synchronous rectifier. The voltage across M_5 (M_6) is clamped at V_2. The current slopes of L_1 is

$$\frac{di_{L1}}{dt}=\frac{V_{cc1}-V_{Ct1}-NV_{Ct2}-NV_2}{NL_1} \tag{5}$$

Where V_{Ct1}, V_{Ct2}, V_{Cc1} are average voltages of Ct1, Ct2, and Cc1, respectively.

Stage 2 (t_1-t_2): M_1 is turned off at t_1. The capacitor in parallel with M_1 is charged linearly and the capacitor in parallel with M_2 is discharged. The stage terminates at t_2, while the voltage across M_2 is zero.

Stage 3 (t_2-t_3): M_2's body diode starts to conduct at t_2. Then M_2 is turned on in zero-voltage condition. The current i_{L1} decreases linearly and its direction is changed from positive to negative. The slope of i_{L1} is

$$\frac{di_{L1}}{dt}=\frac{-V_{Ct1}-NV_{Ct2}-NV_2}{NL_1} \tag{6}$$

Stage 4 (t_3-t_4): At t_3, M_3 (M_4) is turned off. The capacitor in parallel with M_3 (M_4) is charged and the capacitor in parallel with M_5 (M_6) is discharged linearly. At the end of this stage, the voltage across M_4 decreases to zero.

Stage 5 (t_4-t_5): The body diode of M_5 (M_6) is conducting at the beginning of this stage. Therefore M_5 (M_6) is turned on in zero-voltage condition. The slope of i_{L1} is

$$\frac{di_{L1}}{dt}=\frac{-V_{Ct1}-NV_{Ct2}+NV_2}{NL_1} \tag{7}$$

Stage 6 (t_5-t_6): At t_5, M_2 is turned off. The capacitor in parallel with M_2 is charged and the capacitor in parallel with M_1 is discharged linearly. At the end of this stage, the voltage across M_1 goes down to zero.

Stage 7 (t_6-t_7): At the beginning of this stage, the body diode of M_1 is conducting and M_1 is turned on in zero-voltage condition. The slope of i_{L1} is

$$\frac{di_{L1}}{dt}=\frac{V_{Cc1}-V_{Ct1}-NV_{Ct2}+NV_2}{NL_1} \tag{8}$$

Stage 8 (t_7-t_8): At t_7, M_5 (M_6) is turned off. The capacitor in parallel with M_5 (M_6) is charged and the capacitor in parallel with M_3 (M_4) is discharged linearly until the voltage across M_3 reaches zero. After t_8, the next switching cycle starts again.

On the contrary, in the backward mode, the gate drive signals of M_3 (M_4) and M_5 (M_6) are leading to those of M_1 and M_2. The principle of operation of the backward mode (power flows from V_2 to V_1) is similar to that of the forward mode, so it will not be explained in this paper.

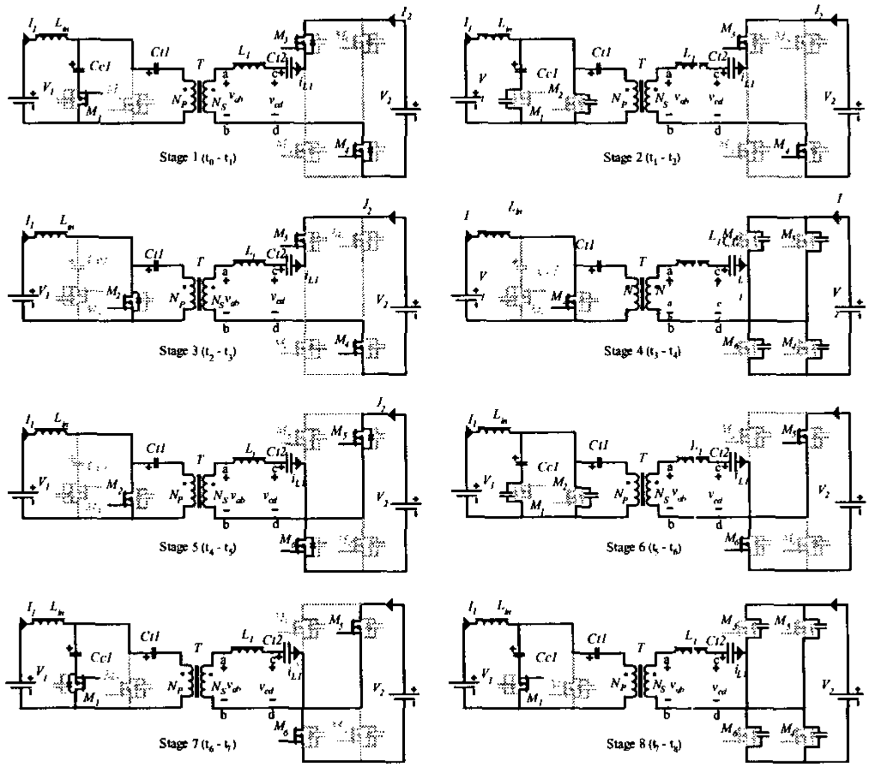

Fig.9. Operation stages of the converter in the forward mode.

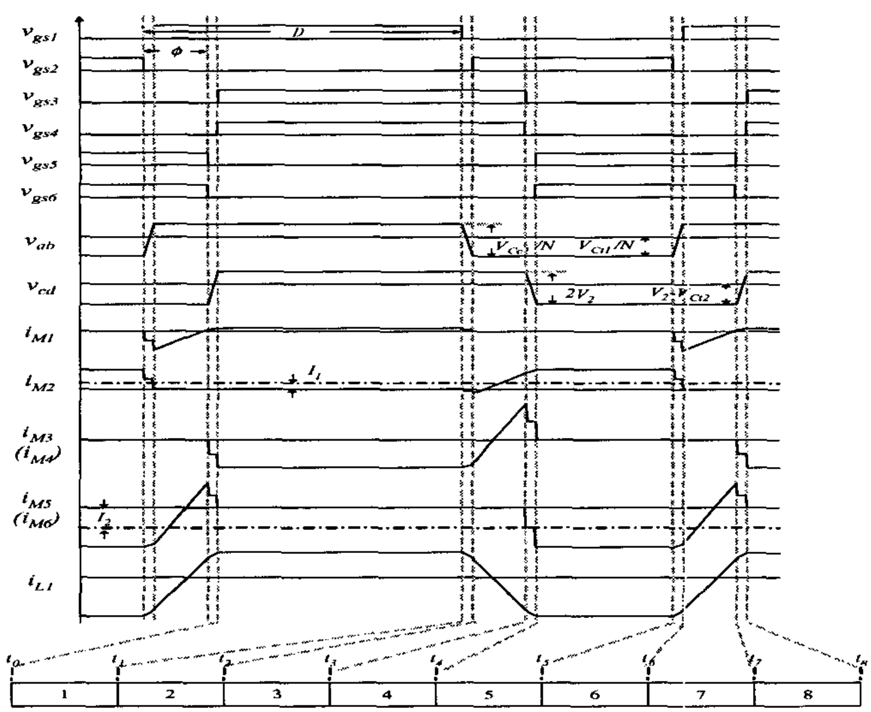

Fig.10. Steady-state waveforms of the converter in the forward mode

V. Experimental and Simulation Results

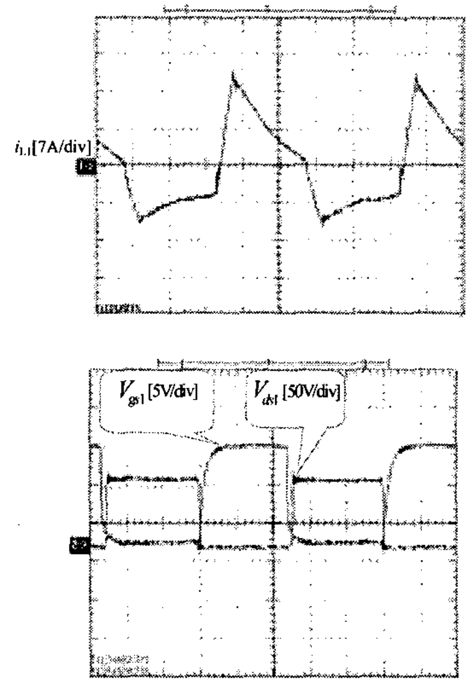

(a) PS control

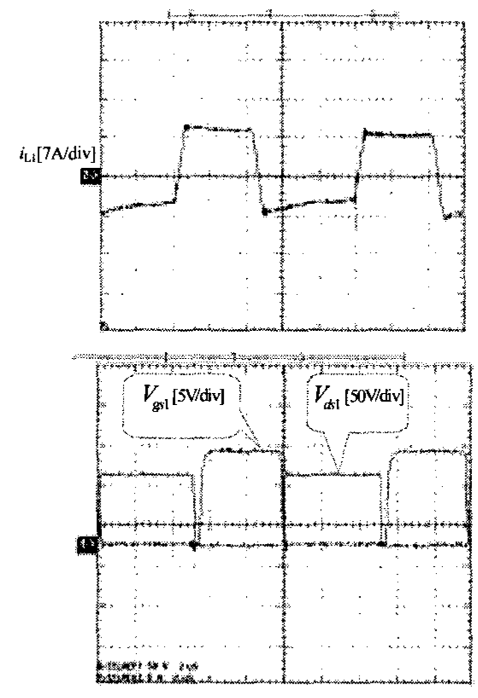

(b) PPS control

Fig.11. Experiment waveforms when V_2 = 16Vdc (50W-output) (2us/div)

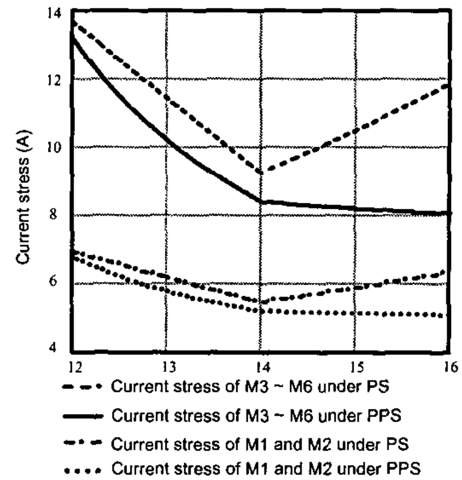

Fig.12. Current stress versus output voltage (V) (100W-output)

A prototype of PPS control bidirectional DC-DC converter shown in Figure 8 is built to verify the analysis. Experiments are performed under the following conditions: V_1=42Vdc, V_2=14Vdc~18Vdc, $Np:Ns$=3:1, L_0=140μH, $Ct1=Ct2$=14.1μF, $Cc1$=4.7μF, L_1=2.8μH , switching frequency f=100kHz.

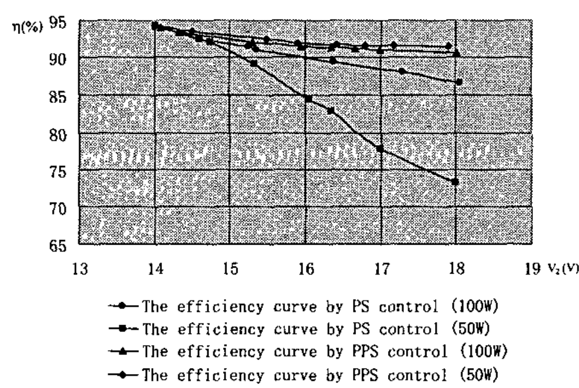

Fig.13. Experimental efficiency waveforms versus output voltage

Fig.11 shows experimental waveforms under V_2=16Vdc with 50W output power condition. The converter under PS control cannot achieve ZVS, while the converter under PPS control can still hold ZVS. Therefore, PPS control can reduce switching loss. Fig.12 show simulation result of current stress versus output voltage, and it can see that the current stress is reduced by PPS control. Fig.13 shows the efficiency curves of the converter under PS and PPS control. It can be easily found that PPS control has higher efficiency than PS control, especially under light-load condition.

VI. Conclusion

PPS control technique combines both phase-shift bidirectional DC-DC converter and the advantage of PWM control and phase-shift control. A technique to synthesize

PWM plus phase-shift bidirectional DC-DC converters topologies is presented. One PPS bidirectional converter is investigated as an example. Theoretical analysis, simulation and experimental results are provided.

ACKNOWLEDGMENT

The authors would like to thank the support of Project Number 50377037 by National Natural Science Foundation of China.

REFERENCES

[1] Hui Li, Peng, F.Z, Lawler, J.S., "A natural ZVS high-power bi-directional DC-DC converter with minimum number of devices". Conference Record of the 2001 IEEE , vol.3,no.30, Sep-4 Oct 2001 ,pp.1874 -1881

[2] Chuanhong Zhao, Dehong Xu, Haifeng Fan, "A PWM plus Phase-Shift Control Bidirectional DC-DC Converter", Applied Power Electronics Conference and Exposition, 2003. APEC '03. Eighteenth Annual IEEE, Volume: 2, 9-13 Feb. 2003, Page(s): 641 -647.

[3] Manu Jain, Praveen K. Jain, and Matteo Daniele, "Analysis of a bidirectional DC-DC converter topology for low power application," IEEE Proc. of CCECE'97, pp. 548-551.

[4] Gang Chen, Dehong Xu, Yousheng Wang, and Yim-Shu Lee, "A New Family of Soft-Switching Phase-shifted Bidirectional DC-DC converters," IEEE Proc. of PESC'01, pp. 859-865

[5] Mustansir H.Kheraluwala and RANDAL.W.Gascoigne, "Performance characterization of a high active bridge dc-to-dc converter", IEEE Trans. Industry Applications,vol. IA-28,no.6,pp. 1294-1301,Nov./Dec.1992